IET Generation, Transmission & Distribution

Controller to Enable the Enhanced Frequency Response Services from a Multi-Electrical Energy Storage System

GTD-2018-5931 | Research Article

Submitted on: 04-07-2018

Submitted by: Francisco Sanchez, Joshua Cayenne, Francisco Gonzalez-Longatt, Jose Luis Rueda

Keywords: ENERGY STORAGE SYSTEM, FREQUENCY RESPONSE, FUZZY LOGIC CONTROLLER, SYSTEM INERTIA

Controller to Enable the Enhanced Frequency Response Services from a Multi-Electrical Energy Storage System

Francisco Sanchez [1*], Joshua Cayenne [2], Francisco Gonzalez-Longatt [1], José Luis Rueda [3]

[1] Centre for Renewable Energy Systems Technology (CREST), Loughborough University, LE11 2HN, Loughborough, United Kingdom
[2] Network Capability-Electricity, National Grid plc, Warwick Technology Park, CV34 6DA, Warwick, United Kingdom
[3] Department of Electrical Sustainable Energy, Delft University of Technology, Delft, Netherlands
[*] f.sanchez@lboro.ac.uk

Abstract: The increased adoption of renewable energy generation is reducing the inertial response of the Great Britain (GB) power system, which translates into larger frequency variations in both transient and pseudo-steady-state operation. To help mitigate this, National Grid (NG), the transmission system operator in GB, has designed a control scheme called Enhanced Frequency Response (EFR) specifically aimed at energy storage systems (ESSs). This paper proposes a control system that enables the provision of EFR services from a multi-electrical energy storage system (M-EESS) and at the same time allows the management of the state of charge (SOC) of each ESS. The proposed control system uses a Fuzzy Logic Controller (FLC) to maintain the SOC as near as possible to the desired SOC of each ESS while providing EFR. The performance of the proposed controller is validated in transient and steady-state domains. Simulation results highlight the benefits of managing the SOC of the energy storage assets with the proposed controller. These benefits include a reduced rate of change of frequency (ROCOF) and frequency nadir following a loss of generation as well as an increase in the service performance measure (SPM) which renders into increased economic benefits for the service provider.

1. Introduction

1.1 Motivation

The electricity generation in Great Britain (GB) has relied on the use of large-scale synchronous machines for over a hundred years. Being synchronised, they contribute to the total system inertia which is provided by their rotating masses. The system inherently maintains a significant amount of inertia that allows frequency control during a power imbalance. Ending the reliance on fossil fuel-based power generation is one of the effective actions against the effects of climate change. Consequently, the traditional thermal plants are being replaced by non-synchronous renewables. However, renewable technologies such as variable speed wind power generation and solar photovoltaic are not synchronously connected to the network. These low-carbon generation technologies use power converters as an interface to the power network, and they are not able to contribute with "natural" inertia in the same way as classical synchronous generators.

There is clear evidence that the total system inertia in GB electrical power system is decreasing due to the growing volume of non-synchronous technologies and the increase in the importing HVDC interconnectors [1]. The lowest recorded total system inertia in the GB power system was 135 GVA.s on 7 August 2016, and it is expected to decrease further under all of the future scenarios [2], GB inertia may be reduced by up to 45% from the current values by 2025.

The reduced inertia makes volatile the system frequency and increases the chance of potential instability arising from system frequency disturbances. Today, the total system inertia of the GB system can be no lower than 130 GVA.s post-fault due to the restriction (0.125 Hz/s) on the post-fault rate of change of frequency (ROCOF) [3] . The higher the ROCOF value is, then the faster is the requirement for the frequency response action.

National Grid plc (NG) is the transmission system operator of GB, and it is responsible for the operation and balancing of the National Electricity Transmission System (NETS) which entails strict control of the system frequency under conditions expressed in the Security and Quality Supply Standards (SQSS) [4].

The conventional frequency control actions operated by NG, are primary, secondary and high-frequency response services. However, NG has identified the need for a new service that must provide both frequency regulation (pre-fault) and frequency containment (post-fault). The new service is called Enhanced Frequency Response (EFR) [5], and NG has designed it in order to utilise the fast response capability of the electrical energy storage (EES) assets (e.g. batteries, flywheels, compressed air systems, etc.) thus improving the capability of the GB system to deal with the consequences of reduced inertia. As the EFR service is mainly aimed at EES assets, it must provide frequency response in one second (or less) after registering a deviation [5]. In a July 2016 EFR tendering exercise, the battery energy storage systems (BESS) was the biggest technology, procuring 201 MW of response with a net cost circa £66 MM [6]. This paper proposes a control system to enable the EFR services from a multi-electrical energy storage system (M-EESS).

1.2 Literature review

Scientific literature regarding primary frequency response (PFR), such as [7–9], are referred to for an overview of the timescales and other dynamic characteristics of the frequency

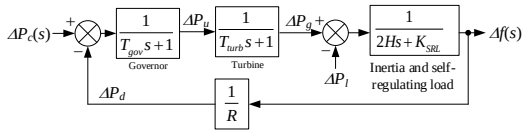

Fig. 1. *Single-area power system: Governor-turbine-generator power system model. Base Case.*

control in an electrical power system. However, the PFR and EFR are very different in several aspects, including the time scale of delivering the service.

Several recent scientific papers have been dedicated to the use of electrical energy storage systems (EESS) to provide PFR; batteries [10, 11], flywheels [12], and electrical vehicles [13]. The use of EESS to provide ancillary services in the electric power system is explored in [14, 15]. These scientific papers provide a useful overview of possible EES technologies but are not focused on how to provide the frequency control in power system applications. However, they identified technologies that could respond quickly enough to the established EFR timescales, e.g. flywheels, batteries, superconducting magnetic energy storage systems and supercapacitors.

The first scientific paper attempting to discuss the novel EFR service is [16], it shows methods to analyse and assess the performance of a single EESS, and power hardware-in-the-loop (HIL) is applied in the real-time network simulations. However, it employs a previous version of the EFR specification making the results outdated. The authors in [17] simulate the provision of EFR by a single BESS responding to a reference set by the system operator. However, only the frequency regulation service is explored and not the post-fault, frequency containment region (in the context of this paper, frequency containment refers to the frequency response provided following a sudden loss of generation or rise in demand to keep the frequency within the limits defined in [4, 18]). In [19], an algorithm is developed to provide EFR while managing the SOC of a single BESS for events in excess of 15 minutes but without including integration of additional EESSs. In [20], simulations are carried out for two storage system topologies, namely a BESS and a combined system of a BESS and a supercapacitor. The authors apply a PI controller to manage the SOC of the storage assets. The studies presented thus far remain narrow in focus dealing mainly with single assets that provide the frequency support service. The present research explores, for the first time, the integration of a multi-electrical energy storage system (M-EESS) for the provision of EFR. Scientific literature reports the use of a variety of control methods for frequency control including classical PID [9] , model predictive control (MPC) [21], and fuzzy logic (FL) or adaptive neuro-fuzzy systems [22]. The specific control of EESS in this domain has been researched in [16]. A fuzzy controller is applied to a battery application in [26], but it is a voltage control application.

1.3 Paper contributions

This study has been one of the first attempts to develop a fuzzy logic controller (FLC) that enables the provision of the novel EFR service by a M-EESS while managing the SOC of its individual assets. The controller is developed using fuzzy-logic because of its simplicity and ease of implementation in a large system containing multiple storage assets. The developed FLC can be easily expanded to accommodate for any number of EESS. Other control methods, such as PID, require a more detailed model of the plant in order to tune the different gains for a specific response. For practical, large systems, it becomes increasingly difficult to obtain an analytical model that accurately represents the dynamics of the system. If the system is subsequently expanded, to include a new energy storage system (ESS) for example, all the gains must be retuned otherwise the system will exhibit poor dynamic performance. The behaviour of the proposed FLC is demonstrated for frequency regulation (pre-fault) as well as for frequency containment (post-fault) operation. The developed FLC can manage the SOC of the storage assets and respond to frequency deviations in line with EFR guidelines, therefore maximising profitability for the service provider. These findings will be of interest to service providers and integrators with a desire to participate in the growing market of energy storage for frequency stability.

1.4 Paper structure

The dynamic model of the power system and the different EES systems models are outlined in Section 2, the EFR service and the proposed FLC for an M-EESS is presented in Section 3. Simulations and results obtained for the different scenarios considered are explained in Section 4, and the concluding remarks are included in Section 5.

2. System Modelling

This section presents the main modelling aspects of the system frequency response (SFR) of a single area power system, and the M-EESS considered in this paper for frequency support. The M-EESS consists of any number and mix of EESSs, for simplicity this paper considers three EESSs: BESS, FESS and UCSS. More detailed EESS models can be used, but to show the essential features of the proposed controller, the models explained in this section are deemed appropriate.

2.1 Single area power system model

A single area power system is considered for simplicity (but the concepts presented here can be extended to a multi-area system), it consists of a single equivalent generation unit fitted with the classical primary frequency control (PFC), as depicted in Fig. 1.

The single area system includes the effects of the inertia and self-regulating load and a generic governor-turbine model; the parameters T_{gov} and T_{turb} are the governor-turbine time constants, respectively. The change in the turbine input power following a frequency variation is given by the frequency droop constant, R. The effect of the secondary frequency control and inter-area power flows are not considered, but they can be easily included [9]. The time-domain frequency response of the inertia and self-regulating load dynamic is represented as in [9] :

$$\Delta P_g(t) - \Delta P_l(t) = 2H\frac{d\Delta f}{dt} + K_{SRL}\Delta f \qquad (1)$$

The above 1st order differential equation defines the dynamic of the system frequency deviation (Δf) when changes in power generation (ΔP_g) or demand (ΔP_l) take

place across the network. H is referred to as the inertia constant of the single-area and its expressed in seconds. The variable K_{SRL} is known as the self-regulating effect of load in per unit/Hz, and it models the variation in consumed power from the frequency sensitive loads ($K_{SRL} = \Delta P_d/\Delta f$).

2.2 Battery Energy Storage System (BESS) model

A generic dynamic model of a Lithium-Ion (Li-ion) battery model is used in this paper. The battery pack equivalent circuit and the related block models are depicted in Fig. 2 (a).

The model takes a power reference signal (P^*_{BESS}), and the previous state of charge (SOC_0) as inputs, with the outputs being the delivered power (P_{BESS}) alongside the battery state of charge (SOC_{BESS}). The charging/discharging dynamic are assumed similar. The battery no-load voltage (E^*_{BESS}) is calculated as a function of the SOC_{BESS}:

$$E^*_{BESS}(t) = E^0_{BESS} + \frac{K_E}{SOC_{BESS}(t)} + \alpha e^{-\beta \int_0^t I_{BESS}(s)ds} \quad (2)$$

where E^0_{BESS} represents the open circuit voltage of the battery pack (V), K_E is defined as the polarisation voltage, α is the exponential zone amplitude of the battery (V) and β is the inverse of the exponential zone time constant (A·h^{-1}). The SOC_{BESS} is calculated as a function of the battery current (I_{BESS}) [27]:

$$SOC_{BESS}(t) = SOC_0 - \frac{1}{Q_{BESS}} \int_{t_0}^{t} I_{BESS}(s)ds \quad (3)$$

where Q_{BESS} is the battery capacity expressed in A·h.

This BESS model is not taking into account thermal or ageing effects of the battery pack, which will affect battery performance in reality [14]. A block in series with the BESS model is included to represent the power converter delay [27], and it also includes logic to protect the battery from certain unrealistic operational conditions, for instance, it will not allow current to flow out when the SOC is zero.

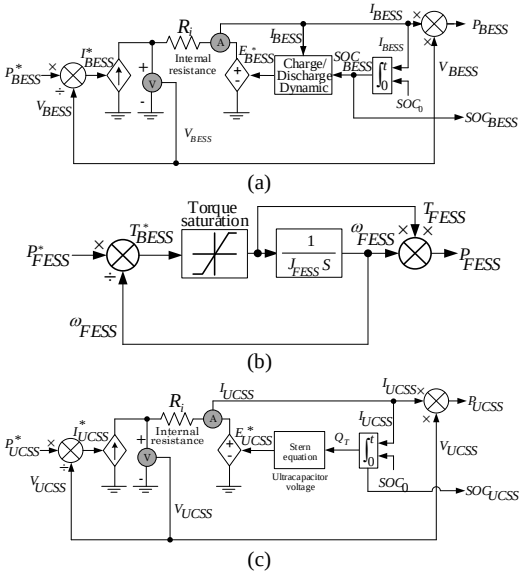

Fig. 2. *Simplified model of a: (a) BESS, (b) FESS, (c) UCSS.*

For many batteries, it is advised to keep the SOC within a certain range in order to reach the expected lifetime of the device [28].

2.3 Flywheel Energy Storage System (FESS) Model

The power given by a flywheel, P_{FESS}, is obtained by computing the product of the torque, T_{FESS}, and the rotational speed, ω_{FESS}, as:

$$P_{FESS} = T_{FESS}\omega_{FESS} \quad (4)$$

The model input is the reference power input (P^*_{FESS}) and the output is the actual delivered power (P_{FESS}), see Fig. 2 (b). The kinetic energy (E_{FESS}) stored in the FESS at a given rotational speed ω_{FESS} (rad/s) is calculated as:

$$E_{FESS} = \frac{1}{2} J_{FESS} \omega^2_{FESS} \quad (5)$$

where J_{FESS} represents the flywheel's inertia constant given in kg·m^2. The electromechanical dynamic of the FESS is modelled by:

$$J_{FESS} \frac{d\omega_{FESS}(t)}{dt} = T^*_{FESS} = -\frac{P^*_{FESS}}{\omega_{FESS}} \quad (6)$$

where P^*_{FESS} is the output power controlled by converter (W). A torque saturation block is implemented because there will be a limited amount of torque (T_{FESS}, N·m) that the flywheel can physically experience [29]. The actual SOC_{FESS} can be derived as:

$$SOC_{FESS}(t) = \frac{\omega^2_{FESS}}{\omega^2_{FESS,\max}} \quad (7)$$

where $\omega_{FESS,max}$, represents the flywheel's system maximum rotational speed (rad/s). For this paper, it was not necessary to include the dynamics of the prime-mover. A block considering the delay introduced by the power converter is also introduced in the model [27]. Further details about FESS modelling including converter characteristics are given in [29], [30].

2.4 Ultracapacitor Storage System (UCSS) Model

Ultracapacitors are also widely known as Supercapacitors or Electric Double Layer Capacitors (EDLCs). The simplified model used in this paper is shown in Fig. 2 (c), and it has similarities to the BESS model. Differences arise principally in characteristics such as the series resistance and the capacitance of the cell. These differences in the parameters of both ESSs indicate that ultracapacitors represent somewhat of a median between the characteristics of capacitors and those of batteries [14]. The UCSS voltage (E^*_{UCSS}) is modelled by the Stern equation (full details of the model can be found on [31], [32]).

The model of each cell is based on an equivalent series resistance (ESR) element and a capacitance in parallel with a leakage resistance branch. A block in cascade with the UCSS model is included to represent the power converter delay, it is a bidirectional power converter which allows power to flow between the ESS and the grid and vice versa. The SOC of the UCSS is calculated according to (8).

$$SOC_{UCSS}(t) = SOC_0 - \frac{1}{Q_{UCSS}} \int_0^t I_{UCSS}(s)ds \quad (8)$$

The initial SOC of the UCSS is denoted by SOC_0 while the UCSS electric charge is denoted by Q_{UCSS} (in Coulomb).

3. EFR and Proposed Controller

The technical specifications for the EFR service are provided by NG and the implementation considering a single EESS used in this paper is explained in the next subsection.

3.1 Enhanced Frequency Response (EFR) Specification

All ESS asset owners must abide by the specifications given in [5] to provide the service and receive compensation. The asset should respond within one second of registering the frequency deviation and must provide its rated power (P_n) for a minimum of 15 minutes. Depending on the value of the frequency deviation (Δf), the response power provided by the ESS assets (P_{EESS}) must change as per the different operating regions shown in Fig. 3. There are two specifications for the EFR service: *wideband* (WB) and *narrowband* (NB). The details of the specific points defining the EFR service envelope are shown in Table 4.

The energy storage asset provides a proportional power response when the frequency deviation is larger than the frequency insensitive band (points W and X of Fig. 3), which is Δf = ±0.05 Hz in the WB service and ±0.015 Hz in the NB service. The EFR service is assumed WB for the explanations in the next sections of the paper. Outside the frequency insensitive band, the EFR controller follows equations (9) - (16) (see Table 5), in which the variable m_{ab} represents the slope of the controller's characteristic (pu/Hz), and the subscripts *a* and *b* represent the frequency deviation identifiers (U, …, Z) as shown in Fig. 3.

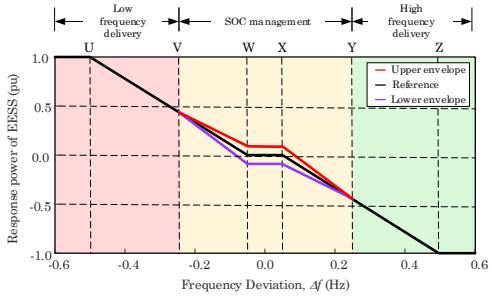

Fig. 3. *Schematic representation of the EFR service and its envelopes. This profile is described in the EFR technical specifications* [5].

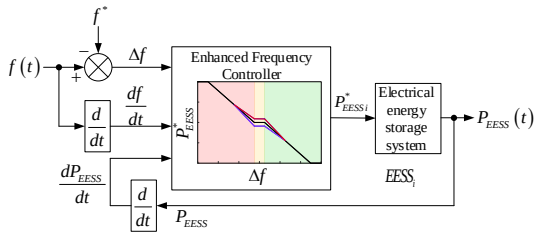

Fig. 4. *EFR controller integrated with the EESS to control output power (P_{EESS}) and ramp rate (dP_{EESS}/dt). f^* is the nominal system frequency (50 Hz).*

The equations (11), (13) and (10), (12) define, respectively, the lower and upper envelopes as shown in Fig. 3. The changes in the system frequency also define the maximum allowable change of the response as a proportion of the capacity of the asset. This limitation has been included to prevent the EESS from producing large frequency deviations by trying to inject large amounts of power too quickly to correct the frequency and thus disrupting the system stability. NG has provided specifications for the minimum and maximum ramp rates in each area of the EFR curve. The maximum ramp rates between points W and X (frequency insensitive band) are established as 0.01 pu/s when the EESS is either discharging to the grid or charging itself. Inside the envelopes (points V and W and X and Y of Fig. 3), the maximum and minimum ramp rate (dP_{EESS}/dt), depends on the value of the ROCOF (df/dt) and its value in pu/s is given by (17).

$$\left(-\frac{1}{0.45}\frac{df}{dt}-0.01\right)\le\frac{dP_{EESS}}{dt}\le\left(-\frac{1}{0.45}\frac{df}{dt}+0.01\right) \quad (9)$$

If the EESS is operating below the lower boundary of the envelope (under-producing), its maximum ramp rate is equal to 2.0pu/s and if it is operating above the upper boundary (over-producing), 0.1pu/s. The fraction of the EESS rated power that should be provided at any given time is given by the control output, P^*_{EESS}. The reference power signal (P^*_{EESS}) from the controller is calculated by computing the gradient on each section, and it depends on the frequency deviation (Δf). A negative value means that the EESS is importing power at the corresponding percentage of its capability. Fig. 4 shows the control structure for the EFR controller which includes the EES system models as well as ramp rate control scheme.

A metric of the of the quality of the EFR has been defined by NG, it is called Service Performance Measure (SPM). The SPM is calculated on a second-by-second basis as the ratio between the response power of ESS (P_{EESS}) against the service envelopes, (10)-(13). If the EESS operates within the specified envelopes, the SPM is 100%. When the EESS operates outside of the specified envelope, it will be penalised with a lower SPM which means a proportional reduction in payment.

3.2 Managing the SOC of EESS: Fuzzy Logic Controller (FLC)

One of the defining characteristics of the EFR service is that it allows the energy providing asset to manage its SOC while its output remains within the service envelope. A Fuzzy Logic Controller (FLC) is developed to manage the SOC of each of the ESS assets when the frequency deviation is within ±0.25 Hz from the nominal frequency as stipulated in the EFR characteristic. As described in the previous subsection, the EFR service profile is bounded between two envelopes for frequencies between points V and Y (see Fig. 3). The envelopes provide the opportunity for those EES assets with a finite energy storage capability (such as the M-EESS technologies focussed on in this paper) to manage their SOC. If the SOC of the asset is lower than its reference value, the FLC instructs it to charge or discharge following the lower EFR envelope. Conversely, if the SOC of the asset is higher than its reference value, the FLC instructs it to charge or

discharge following the upper EFR envelope. The middle service reference is expected to be followed by demand-side providers of the EFR service who cannot manage their SOC. If the frequency deviation is larger than ±0.25 Hz, the envelope becomes a single line as this is considered post-fault. In this case, the assets do not have the freedom to manage their SOC and must follow the single reference line to assist the grid. This paper proposes a controller to enable the provision of EFR services from a Multi-EESS (M-EESS). The proposed FLC consists of two inputs namely the frequency deviation (Δf) and the error in the state of charge ($SOC_{e,i}$) of each EESS asset ($EESS_i$), and one output, which corresponds to the power output targets for each asset ($P^{FLC}{}_i$). The error in the asset's SOC is obtained by subtracting the measured value from the reference or target ($SOC^*{}_i$). In this case, a negative value of $SOC_{e,i}$ is obtained when an ESS has more stored energy than required and the opposite is true for a positive value of $SOC_{e,i}$.

Fig. 5 shows a simple block diagram of the generic FLC proposed to provide the EFR service, indicating the main functionalities. The EFR controller limits the output power as well as the ramp rates of the assets to comply with the technical requirements specified in Section 3.1 above. Because the EFR provider needs to be able to inject, as well as absorb energy from the grid depending on the value of the frequency deviation, an ideal SOC to maintain would be 50% [33]. From the EFR provider's point of view, choosing an optimum SOC, in line with the particularities of their own EESS system, while at the same time providing an adequate EFR service would constitute a highly desirable operation (the optimal selection of the SOC is beyond the scope of this paper).

3.2.1 Membership Functions and Rule Base of the FLC: The control system based on fuzzy logic is chosen because of the easy implementation of rules and its implementation on applications where obtaining a complete analytic model of the system is difficult. Also, the categorisation of operating ranges of EESS into membership functions gives the flexibility to manage their power injections/absorptions and to align them with the needs of the system. Overall, the design of the FLC has utilised the methodologies discussed in [34] as a starting approach. However, common sense, operational experience and expert judgement have been applied in designing the controller for the EES application. The flexibility and adaptability that the FLC provides is something very valuable which enables the designer to quickly modify input parameters and observe the change in the output.

The membership functions (MF) must be carefully selected for the controller to fulfil the desired control target, the shape of which depends on the chance variation of the variable [35]. Triangular membership functions are used in the proposed FLC because they provide a good indication of the linguistic values graphically and this way its relatively straightforward to design and modify.

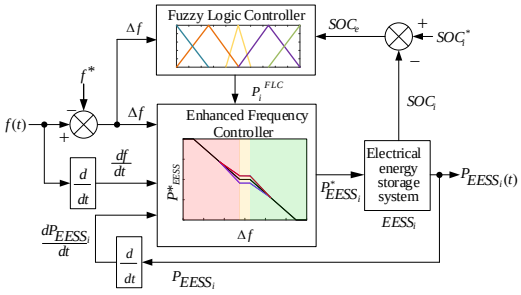

Fig. 5. *Proposed FLC to enable EFR services from Multi-EESS.*

Also, it does not require definition or tuning of several parameters. In the fuzzification stage, Δf and $SOC_{e,i}$ are transformed into linguistic values. Therefore it is necessary to apply MFs to analyse the magnitudes of Δf and $SOC_{e,i}$. The magnitude represents the degree in which a numerical input value is a member of each linguistic variable.

The "Positive" (P) and "Large Positive" (LP) variables require different control action, but a larger resolution can be opted for with appropriate results for this application. The same applies to the "Negative" (N) and "Large Negative" (LN) MFs. The same linguistic variables are given to both the inputs and outputs to maintain a consistent framework. The shape of the input or output membership functions and the parameters of each linguistic variable can be modified if deemed necessary to change the output behaviour of the FLC.

Fig. 6 shows the MFs associated with (a) Δf, (b) $SOC_{e,i}$ and (c) output reference power (P^{FLC}). A high-resolution term can be useful when the frequency dead band is narrow. Therefore, for the FLC frequency input variable is shown in Fig. 6 (a), the membership function representing "zero deviation" (Z) is narrower than the other membership functions. The same applies to the SOC error input variable.

The optimum power output for each of the EES assets is identified by the rule base of the FLC. Each of the outputs implements its rules based on the state of two inputs, the corresponding SOC error for each asset and the frequency deviation. The rule base of the FLC is shown in Table 1, and a surface view of this rule base is depicted in Fig. 7.

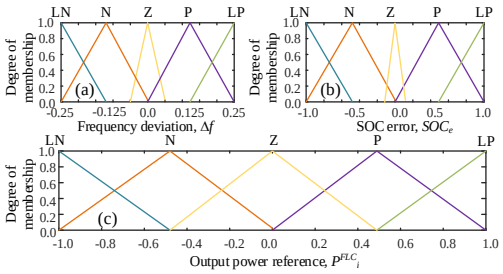

Fig. 6. *Membership function associated with (a) frequency deviation Δf, (b) SOC error (SOC_e) and (c) output reference power ($P^{FLC}{}_i$) provided to each ESS model. $P^{FLC}{}_i < 0$, charging; and $P^{FLC}{}_i > 0$, discharging.*

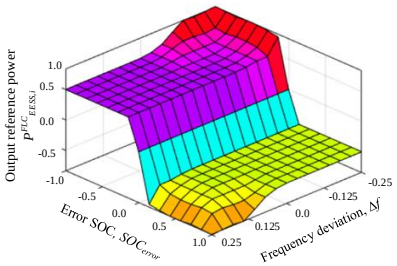

Fig. 7. *Surface view of the rule base for the proposed FLC to enable EFR services from a M-EESS.*

Table 1. Rule base of the FLC to determine the output of the FLC using the linguistic variables of Δf and SOC_e. LN: "Large Negative", N: "Negative", Z: "Zero", P: "Positive", LP: "Large Positive".

		Frequency deviation, Δf				
		LN	N	Z	P	LP
SOC error SOC_e	LN	LP	LP	P	P	P
	N	LP	P	P	P	P
	Z	Z	Z	Z	Z	Z
	P	N	N	N	N	LN
	LP	N	N	N	LN	LN

In this paper, the output membership functions of the ESSs are similar, but if necessary, their characteristics (i.e. numerical range and slopes) could be adapted to the specified operation of an EFR provider's asset.

4. Simulations and Results

The performance of the proposed controller to provide EFR services with a M-EESS is analysed in this section. Two simulation cases are considered: *Case I*: A single area system, representative of the GB power system for the year 2025 is subjected to a sudden disconnection of a large generator, allowing the observation of the M-EESS providing both variants of the EFR service. *Case II*: a 12-hour time series of frequency data from the GB system, provided by NG [3], is used to evaluate the performance of the proposed FLC and the provision of regulation services while managing the SOC of the M-EESS; for this case two scenarios are considered: *Scenario II.A:* The M-EESS provides EFR and the SOC is unmanaged; Scenario *II.B:* The M-EESS provides EFR and the SOC is managed by the FLC.

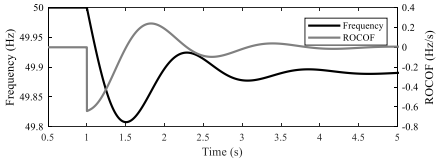

Fig. 8. *Time-domain response of system frequency [Hz] and ROCOF [Hz/s] following a loss of 1,800 MW of generation.*

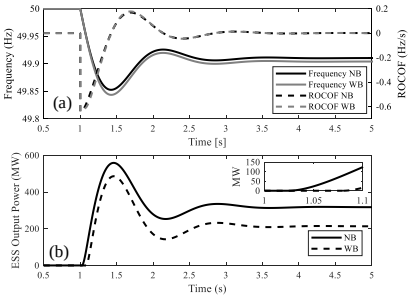

Fig. 9. *System's response after a loss of 1,800 MW of generation. M-EESS providing NB and WB EFR service: (a) Frequency and ROCOF, and (b) EESS output power, P_{EESS} (combined power of M-EESS).*

Table 2. Summary of main performance indicators: *Case I.*

Indicator	*Base Case*	*M-EESS*	
		NB	*WB*
Steady State Frequency, f_{ss} (Hz)	49.891	49.91	49.90
Frequency Nadir, f_{min} (Hz)	49.808	49.85	49.84
Time of frequency Nadir, t_{min} (s)	1.510	1.439	1.443
$ROCOF_{max}$ (Hz/s)	-0.6427	-0.6424	-0.6424
SPM (%)	N/A	100.00	100.00

The key response indicators are summarized in Table 3, where SOC_{Ref} represents the reference SOC of the ESS which is set by the operator and is managed by the FLC. SOC_0 and SOC_F represent the SOC of the ESS at the instant starting to provide the EFR service and at the end of the time series respectively. In both cases, an SPM value of 100% is achieved. Finally, E represents the energy supplied to the grid by the ESSS in MWh.

4.1 Case I: Single Area System representative GB system 2025 subject to a large disturbance

A single area system, representative of a single machine equivalent of the GB system for the year 2025 is used for illustrative purposes. The stored kinetic energy in the rotating elements of the system is 70 GJ. This value is derived from NG lowest estimated inertia for the year 2025 [2]. The self-regulating load component (K_{SRL}) is assumed at 0.05 pu/Hz [3]. The system's base for per unit calculations is 30.0 GW. The frequency response model of the test system includes only the primary speed governor control. The time constants of the turbine (T_t) and governor (T_g) are chosen as 0.3 s, and 0.08 s respectively [9] .

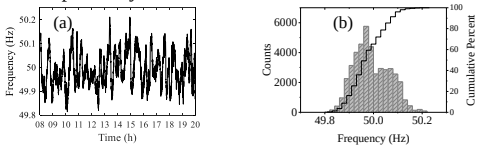

Fig. 10 *(a) Time-domain representation of 12-hour frequency sample from NG, (b) Histogram and discrete CDF of frequency time series.*

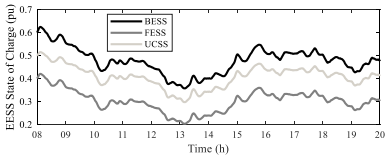

Fig. 11. *Time-domain plot of the SOC of each EESS following the NG 12-hour frequency sample: Scenario II.A.*

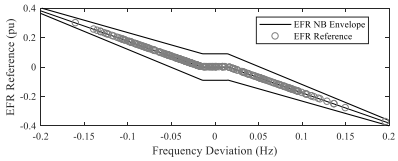

Fig. 12. *EFR Reference Signal to BESS within EFR NB service envelope and with no SOC management.*

The speed-droop regulation constant of the governor is given a value of R = 2.0 Hz/pu [18]. The initial SOC of the assets (SOC_0) is set at 50%. The system frequency response (SFR) of the test system without any M-EESS (*Base Case*) is analysed with the infrequent infeed loss risk value of 1,800 MW [4] (ΔP_g = -0.06 pu), and it is shown in Fig. 8. Fig 9 shows the SFR of the single area system considering an M-EESS providing EFR service for the same loss of generation. A summary of the main performance indicators is shown in Table 2.

The numerical results indicate that, due to the reduced size of the frequency insensitive band, the NB service begins injecting power to the system before the WB service, (see Fig. 9 (a)). The maximum power injected ($P_{EESS,max}$) in the NB service is higher than that provided by the WB service, as depicted in Fig. 9 (b).

4.2 Case II: Small deviation of the system's frequency

NG has released GB system frequency data from January 2014 to December 2015, with one-second resolution, in order to allow the analysis of the EFR services by potential providers [5]. Fig. 10 (a) shows a time-domain plot of a 12-hour sample of the NG frequency data corresponding to 05 of January 2014, which is used to test the EFR controller providing the NB service. Fig. 10 (b) shows the histogram and discrete cumulative distribution function (CDF) of the frequency time series. The frequency is below the nominal value for 59.34% of the selected 12-hour period. The initial SOC of the assets has been selected as 60 % for the BESS, 50 % for the UCSS and 40 % for the FESS.

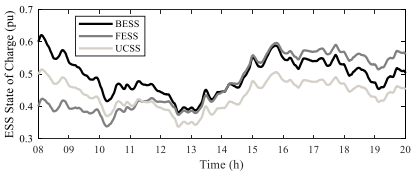

Fig. 13. *Time-domain plot of the SOC of each EESS following the NG 12-hour frequency sample: Scenario II.B.*

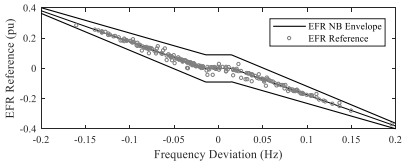

Fig. 14. *EFR Reference Signal to BESS within NB service envelope and with SOC managed by the FLC.*

Table 3. Summary of results for the *Case II.*

EESS	*Indicator*	*Scenario II.A*	*Scenario II.B*
BESS	SOC_0	0.60	0.60
	SOC_F	0.48	0.50
	SOC^*	N/A	0.50
	E [MWh]	203.47	156.16
UCSS	SOC_0	0.50	0.50
	SOC_F	0.41	0.45
	SOC^*	N/A	0.45
	E [MWh]	1.02	0.57
FESS	SOC_0	0.40	0.40
	SOC_F	0.30	0.56
	SOC^*	N/A	0.6
	E [MWh]	5.09	-8.39
M-EESS	E [MWh]	209.57	148.35
	SPM [%]	100	100

4.2.1 Scenario II.A: M-EESS is enabled to provide EFR, and the SOC is unmanaged: The average SOC of each EESS decreased by 10% after the 12-hour period (see Fig. 11). The total net energy that the M-EESS provided to the system during the 12-h period is 209.6 MWh. As shown in Fig. 10 (b), the frequency sample spends more time below 50 Hz. Therefore, the M-EESS tends to provide more energy to the grid than the energy drawn from the grid for recharging.

To verify the correct operation of the EFR controller, the reference signal applied to the BESS is plotted against each value of the frequency in the 12-hour sample from NG (see Fig. 12). It is apparent from this figure that all points are located inside the EFR NB envelope, demonstrating the appropriate performance of the controller. All points lie on the reference line since there is no SOC management. Because the reference points all lie within the service envelope, an SPM of 100% is achieved.

4.2.2 Scenario II.B: M-EESS is enabled to provide EFR, and the FLC manages the SOC: Like in the previous scenario, the ramp limitations are imposed for the delivered power. The initial SOC values for the M-EESS are the same as those used for the previous scenario whereas the reference SOC values are 50 % for the BESS, 45 % for the UCSS and 60 % for the FESS (see Table 3). The FESS is biased towards charging and both the BESS and UCSS are biased towards discharging given their initial SOC.

The SOC of all three storage assets evolves towards the appropriate reference values, validating the operation of the FLC (see Fig. 13). For this scenario, the ESS behaved like a net exporter of energy with a total of 148.35 MWh injected during the 12-hour period. It follows then that including the

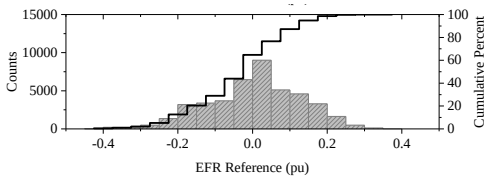

Fig. 15. *Histogram and discrete CDF of EFR reference signal applied to BESS: Scenario II.B.*

FLC helps the asset operator in the management of the M-EESS while conforming with the EFR guidelines. To verify the correct operation of the controllers, the EFR reference signal to the BESS, for each value of the frequency deviation in the 12-hour sample from NG, is plotted in Fig. 14. The reference signal points all lie within the service envelope, thereby producing an SPM of 100%, but they are not exactly in the service reference since in this case, the FLC is managing the SOC of the BESS. Fig. 15 shows the histogram and discrete CDF of the EFR reference signal applied to the BESS.

4.2.3 Discussion: In Scenario II.A, the SOC of each ESS decreases by 10% on average. This is because its response follows the middle reference line of the EFR service without regards for its SOC. On the other hand, in Scenario II.B, the SOC of each ESS increases or decreases depending on its desired value while providing the EFR service managed by the FLC. This scenario exhibits less dispersion in the EFR reference signals due to the action of the FLC.

5. Conclusions

This paper shows the development of a controller to facilitate a M-EESS providing the EFR service. The FLC improved the ESS ability to manage its SOC, which is valuable for assets with finite energy delivery capabilities. The developed FLC is simple to implement and it does not lessen the quality of the EFR delivered by the ESS, as restrictions are applied to the control signal to maintain the output power within the service envelope boundaries. This means that higher values of SPM are achieved which renders an increased economic remuneration for the provider. The solution presented in this paper is demonstrated in a single area power system model with speed governors having the same droop coefficient. The same controller could be applied to a single area system with generators modelled to have different speed-droop constants. Also, the controller could be applied inside a multi-area power system model connected by tie lines. Advancement of this research would be to use narrow-topped trapezoids instead of triangular membership functions for the FLC. Additionally, statistical analysis of the input variables could be undertaken to define the dimensions of each trapezoid. The existing FLC-based solution could be improved to include learning elements by combining neural networks to make an adaptive neuro-fuzzy inference system (ANFIS) controller. Currently, the membership functions have been chosen and therefore, are fixed; ANFIS controllers would remove the need for "expert" knowledge in the design.

6. References

[1] Ashton, P.M., Saunders, C.S., Taylor, G.A., Carter, A.M., Bradley, M.E.: 'Inertia estimation of the GB power system using synchrophasor measurements'*IEEE Trans. Power Syst.*, 2015, **30**, (2), pp. 701–709.

[2] National Grid: 'Future Energy Scenarios' (2017). Available: http://fes.nationalgrid.com/fes-document/fes-2017/, accessed 15 January 2018

[3] National Grid: 'System Operability Framework 2016' (2016). Available: https://www.nationalgrid.com/uk/publications/system-operability-framework-sof, accessed 15 January 2018

[4] National Grid: 'National Electricity Transmission System Security and Quality of Supply Standard'2017, **Ver. 2.3**, (March), p. 59. Available: https://www.nationalgrid.com/uk/electricity/codes/security-and-quality-supply-standards, accessed 13 December 2017

[5] National Grid: 'Enhanced Frequency Response' (2016). Available: https://www.nationalgrid.com/uk/electricity/balancing-services/frequency-response-services/enhanced-frequency-response-efr, accessed 04 July 2018

[6] National Grid: 'Enhanced Frequency Response Market Information Report' (2016). Available: https://www.nationalgrid.com/uk/electricity/balancing-services/frequency-response-services/enhanced-frequency-response-efr?market-information, accessed 04 July 2018

[7] Ela, E., Gevorgian, V., Tuohy, A., Kirby, B., Milligan, M., O 'malley, M.: 'Market Designs for the Primary Frequency Response Ancillary Service—Part I: Motivation and Design'*IEEE Trans. POWER Syst.*, 2014, **29**, (1).

[8] Machowski, J., Bialek, J.W., Bumby, J.R.: 'Power system dynamics : stability and control' (John Wiley, 2008, 2nd ed.)

[9] Bevrani, H.: 'Real Power Compensation and Frequency Control', in 'Robust Power System Frequency Control' (Springer US, 2009), pp. 1–23

[10] Stroe, D.I., Knap, V., Swierczynski, M., Stroe, A.I., Teodorescu, R.: 'Suggested operation of grid-connected lithium-ion battery energy storage system for primary frequency regulation: Lifetime perspective', in '2015 IEEE Energy Conversion Congress and Exposition, ECCE 2015' (IEEE, 2015), pp. 1105–1111

[11] Swierczynski, M., Stroe, D.I., Stan, A.I., Teodorescu, R.: 'Primary frequency regulation with Li-ion battery energy storage system: A case study for Denmark', in '2013 IEEE ECCE Asia Downunder - 5th IEEE Annual International Energy Conversion Congress and Exhibition, IEEE ECCE Asia 2013' (IEEE, 2013), pp. 487–492

[12] Zhang, F., Tokombayev, M., Song, Y., Gross, G.: 'Effective flywheel energy storage (FES) offer strategies for frequency regulation service provision', in 'Proceedings - 2014 Power Systems Computation Conference, PSCC 2014' (IEEE, 2014), pp. 1–7

[13] Izadkhast, S., Garcia-Gonzalez, P., Frias, P.: 'An Aggregate Model of Plug-In Electric Vehicles for Primary Frequency Control'*IEEE Trans. Power Syst.*, 2015, **30**, (3), pp. 1475–1482.

[14] Luo, X., Wang, J., Dooner, M., Clarke, J.: 'Overview of current development in electrical energy storage technologies and the application potential in power system operation'*Appl. Energy*, 2015, **137**, pp. 511–536.

[15] Farhadi, M., Mohammed, O.: 'Energy Storage Technologies for High-Power Applications', in 'IEEE Transactions on Industry Applications' (2016)

[16] Greenwood, D.M., Lim, K.Y., Patsios, C., Lyons, P.F., Lim, Y.S., Taylor, P.C.: 'Frequency response services designed for energy storage'*Appl. Energy*, 2017, **203**, pp. 115–127.

[17] Canevese, S., Cirio, D., Gatti, A., Rapizza, M., Micolano, E., Pellegrino, L.: 'Simulation of enhanced frequency response by battery storage systems: The UK versus the continental Europe system'*Conf. Proc. - 2017 17th IEEE Int. Conf. Environ. Electr. Eng. 2017 1st IEEE Ind. Commer. Power Syst. Eur. EEEIC / I CPS Eur. 2017*, 2017, (December 2015), pp. 1–6.

[18] National Grid, Transmission, Britain, G., Act, P.: 'The grid code'2015. Available: https://www.nationalgrid.com/uk/electricity/codes/grid-code. Accessed 06 October 2017

[19] Mantar Gundogdu, B., Nejad, S., Gladwin, D.T., Foster, M., Stone, D.: 'A Battery Energy Management Strategy for UK Enhanced Frequency Response and Triad Avoidance'*IEEE Trans. Ind. Electron.*, 2018.

[20] Bahloul, M., Khadem, S.K.: 'Design and control of energy storage system for enhanced frequency response grid service', in '2018 IEEE International Conference on Industrial Technology (ICIT)' (IEEE,

2018), pp. 1189–1194
[21] Mai Ersdal, A., Cecílio, I.M., Fabozzi, D., Imsland, L., Thornhill, N.F.: 'Applying Model Predictive Control to Power System Frequency Control', in 'Innovative Smart Grid Technologies Europe' (2013), pp. 1–5
[22] Nath, V., Sambariya, D.K.: 'Design and performance analysis of adaptive neuro fuzzy controller for load frequency control of multi-area power system', in 'International Conference on Intelligent Systems and Control' (2016), pp. 1–7
[23] Adrees, A., Milanović, J. V: 'Study of frequency response in power system with renewable generation and energy storage', in 'Power Systems Computation Conference' (2016), pp. 1–7
[24] Jha, I.S., Sen, S., Tiwari, M., Singh, M.K.: 'Control Strategy for Frequency Regulation using Battery Energy Storage with Optimal Utilization', in 'India International Conference on Power Electronics' (2014), pp. 1–4
[25] Serban, I., Marinescu, C.: 'Control strategy of three-phase battery energy storage systems for frequency support in microgrids and with uninterrupted supply of local loads'*IEEE Trans. Power Electron.*, 2014, **29**, (9), pp. 5010–5020.
[26] Anand, R., Mary, P.M.: 'Comparison of PID and Fuzzy Controlled DC to DC Converter with Inductor Resistance'*Int. J. Eng. Sci. Res. Technol.*, 2013, **2**, (8).
[27] Sabah Sami, S., Cheng, M., Wu, J.: 'Modelling and Control of Multi-type Grid-scale Energy Storage for Power System Frequency Response', in '2016 IEEE 8th International Power Electronics and Motion Control Conference (IPEMC-ECCE Asia)' (2016), pp. 269–273
[28] Namor, E., Torregrossa, D., Sossan, F., Cherkaoui, R., Paolone, M.: 'Assessment of battery ageing and implementation of an ageing aware control strategy for a load leveling application of a lithium titanate battery energy storage system', in '2016 IEEE 17th Workshop on Control and Modeling for Power Electronics, COMPEL 2016' (2016), pp. 1–6
[29] Diaz-Gonzalez, F., Bianchi, F.D., Sumper, A., Gomis-Bellmunt, O.: 'Control of a Flywheel Energy Storage System for Power Smoothing in Wind Power Plants'*Energy Conversion, IEEE Trans.*, 2014, **29**, (1), pp. 204–214.
[30] Yuan, H., Jiang, X., Wang, Q., Li, J.: 'Optimization Control of Large-Capacity High-Speed Flywheel Energy Storage Systems', in 'International Symposium on Computer, Consumer and Control' (2016), pp. 1111–1114
[31] Oldham, K.B.: 'A Gouy–Chapman–Stern model of the double layer at a (metal)/(ionic liquid) interface'*J. Electroanal. Chem.*, 2008, **613**, (2), pp. 131–138.
[32] Xu, N., Riley, J.: 'Nonlinear analysis of a classical system: The double-layer capacitor'*Electrochem. commun.*, 2011, **13**, (10), pp. 1077–1081.
[33] Knap, V., Chaudhary, S.K., Stroe, D.I., Swierczynski, M., Craciun, B.I., Teodorescu, R.: 'Sizing of an energy storage system for grid inertial response and primary frequency reserve'*IEEE Trans. Power Syst.*, 2016, **31**, (5), pp. 3447–3456.
[34] Garibaldi, J.M., John, R.I.: 'Choosing Membership Functions of Linguistic Terms', in 'The 12th IEEE International Conference on Fuzzy Systems' (2003), pp. 578–583
[35] Ross, T.J.: 'Fuzzy Logic with Engineering Applications'*IEEE Trans. Inf. Theory*, 2004, **58**, (3), pp. 1–19.

7. Appendices

Table 4. EFR Reference Values for Both the WB and NB Service.

Point	*Wide band*		*Narrow band*	
	Freq. deviation Δf *(Hz)*	*Response Power* P^*_{EESS} *(pu)*	*Freq. deviation* Δf *(Hz)*	*Response Power* P^*_{EESS} *(pu)*
U	-0.500	+1.0000	-0.500	+1.0000
V	-0.250	+0.444444	-0.250	+0.484536
W	-0.050	+0.09 (max)	-0.015	+0.09 (max)
X	+0.050	-0.09 (min)	+0.015	-0.09 (min)
Y	+0.250	-0.444444	+0.250	-0.484536
Z	+0.500	-1.0000	+0.500	-1.0000

Table 5. Explicit WB definitions of EFR service.

Frequency deviation, Δf *(Hz)*	*Response power of EESS,* P_{EESS} *(pu)*	*Equation*
$\Delta f \le -0.50$	$P^*_{EESS} = +1.00$ (max delivery)	(10)
$-0.50 < \Delta f \le -0.25$	$P^*_{EESS} = m_{UV}(\Delta f - f_V) + P_V$ (post-fault)	(11)
$-0.25 < \Delta f \le -0.05$	$P^{max}_{EESS} = m^{max}_{VW}(\Delta f - f_W) + P^{max}_W$ (upper)	(12)
	$P^{min}_{EESS} = m^{min}_{XY}(\Delta f - f_X) + P^{min}_W$ (lower)	(13)
$0.05 \le \Delta f < 0.25$	$P^{max}_{EESS} = m^{max}_{XY}(\Delta f - f_W) + P^{max}_X$ (upper)	(14)
	$P^{min}_{EESS} = m^{min}_{XY}(\Delta f - f_X) + P^{min}_X$ (lower)	(15)
$+0.25 < \Delta f \le +0.50$	$P^*_{EESS} = m_{YZ}(\Delta f - f_Y) + P_Y$ (post-fault)	(16)
$\Delta f \ge +0.50$	$P^*_{EESS} = -1.00$ (max delivery)	(17)